Controlled-valence properties of $La_{1-x}Sr_xFeO_3$ and $La_{1-x}Sr_xMnO_3$ studied by soft-x-ray absorption spectroscopy

M. Abbate, F. M. F. de Groot, and J. C. Fuggle
Research Institute for Materials, University of Nijmegen, Toernooiveld, 6525 ED Nijmegen, The Netherlands

A. Fujimori
Department of Physics, University of Tokyo, 7-3-1 Hongo, Bunkyo-ku, Tokyo 113, Japan

O. Strebel, F. Lopez, M. Domke, and G. Kaindl
Institut für Experimentalphysik, Freie Universität Berlin, Arnimallee 14, D-1000 Berlin 33, Germany

G. A. Sawatzky
Materials Science Centre, University of Groningen, Nijenborgh 18, 9747 AG Groningen, The Netherlands

M. Takano
Institute for Chemical Research, Kyoto University, Uji, Kyoto 611, Japan

Y. Takeda
Department of Chemistry, Mie University, Tsu 514, Japan

H. Eisaki and S. Uchida
Department of Applied Physics, University of Tokyo, Bunkyo-ku, Tokyo 113, Japan
(Received 13 December 1991)

The controlled-valence properties of $La_{1-x}Sr_xFeO_3$ and $La_{1-x}Sr_xMnO_3$ are studied by means of soft-x-ray absorption spectroscopy. A comparison between the transition-metal $2p$ spectra and atomic-multiplet calculations is used to determine the $3d$ count. The O $1s$ spectrum is used to characterize changes in unoccupied states that contain oxygen p character. The results indicate that the holes induced by substitution for both series are located in states of mixed metal $3d$–oxygen $2p$ character. The ground state of $LaFeO_3$ is mainly $3d^5$ and becomes $3d^5\underline{L}$ (where $\underline{L}$ denotes a ligand hole) in the $La_{1-x}Sr_xFeO_3$ series for low Sr concentration. The main component of the ground state of $LaMnO_3$ is $3d^4$ and becomes a mixture of $3d^3$ and $3d^4\underline{L}$ in the $La_{1-x}Sr_xMnO_3$ series. The trends in controlled-valence properties of similar oxides across the transition-metal series can be rationalized within the framework of the Zaanen-Sawatzky-Allen model.

I. INTRODUCTION

Controlled-valence materials like $La_{1-x}Sr_xMO_3$ (where M is a first-row transition metal) show very interesting changes in their physical and chemical properties as a function of composition.[1–4] It was generally assumed that replacement of La^{3+} by Sr^{2+} in these materials would lead to changes in the $3d$ electronic configuration, thereby providing a means to control the valency of the transition-metal ions. This assumption was based implicitly on the idea that oxygen is strongly electronegative and, by comparison, the $3d$ electrons can be easily ionized. However, such a model is naive and can even give rise to wrong predictions for the late transition-metal oxides. This failure as well as the general interest in these materials justify a more detailed investigation of electronic-structure changes as a function of substitution.

One of the main questions to be answered is *which valency is being controlled?* To answer this question, soft-x-ray absorption spectroscopy (XAS) is an ideal tool due to its site- and symmetry-selective character.[5] This potential has been illustrated by numerous XAS and the related electron-energy-loss spectroscopy (EELS) studies of high-T_c superconductors (see, e.g., Ref. 6). It was shown recently that the extra charges induced by substitution in early-transition-metal oxides go to states of primarily transition-metal $3d$ character.[7] This behavior contrasts strongly with that found in most late-transition-metal oxides, where the holes induced by doping go to states which have predominantly O $2p$ character.[8–10] Intermediate controlled-valence materials, with transition metal in the middle of the row, are expected to reflect the crossover, and even intermediate situations can be envisaged, where the extra charges go to states of mixed transition-metal $3d$–oxygen $2p$ character. The purpose of this paper is to explore the behavior of intermediate $La_{1-x}Sr_xFeO_3$ and $La_{1-x}Sr_xMnO_3$ by means of high-resolution O $1s$ and M $2p$ x-ray absorption spectroscopy.

The information provided by the oxygen 1*s* and the transition-metal 2*p* x-ray absorption spectra is complementary and well suited to answer the above question. The most intense structure in the transition-metal 2*p* spectra corresponds to transitions of the form $2p \rightarrow 3d$, as dictated by the dipole selection rule.[5] Transitions of the form $2p \rightarrow 4s$, although much weaker, are also allowed and contribute, in part, to the relatively smooth background observed at higher energies. The $2p \rightarrow 3d$ spectra are dominated by strong multiplet effects due to Coulomb and exchange interactions between the 2*p* core hole and the 3*d* electrons in the final states, which are large as compared to the dispersion of the 3*d* bands in these materials. The peak shapes and chemical shifts are very sensitive to the 3*d* ground-state configuration as well as the crystal-field interactions, and can be used to determine the 3*d* occupancy of the transition-metal ions.[11]

On the other hand, the O 1*s* spectra correspond to transitions to unoccupied oxygen *p* character.[5] The mere existence of such transitions illustrates the partially covalent nature of the bonding in these compounds.[12] Multiplet effects are less important here and the spectra are usually interpreted on the basis of partial density-of-states (DOS) calculations. The O 1*s* spectra map mainly the unoccupied electronic structure at the metal sites, since the O 2*p* character is hybridized with metal states, forming empty bands of predominantly metal weight above the Fermi level. This approach was illustrated by Grioni *et al.*[13] for the O 1*s* spectra of CuO.

All the compounds studied here[14] have slightly deformed perovskite structures, where the crystal fields at the transition-metal sites have approximately octahedral symmetry. $LaFeO_3$ is an antiferromagnetic insulator ($T_N \approx 750$ K), whereas antiferromagnetic $SrFeO_3$ ($T_N \approx 130$ K) has a temperature-independent resistivity. $LaMnO_3$ is an antiferromagnetic insulator ($T_N \approx 100$ K) exhibiting a cooperative Jahn-Teller distortion that removes the degeneracy of the e_g levels by lowering the total electronic energy. $LaMnO_3$ undergoes also a phase transition at $T_t \approx 875$ K from a distorted rhombohedral symmetry to an orthorhombic structure. For certain intermediate compositions, $La_{1-x}Sr_xMnO_3$ is a ferromagnetic metal, but $SrMnO_3$, the other end member of the series, is again characterized as an antiferromagnetic insulator.

II. EXPERIMENTAL DETAILS

The measurements were carried out at the Berliner Elektronen Speicherring-Gesellschaft für Synchrotronstrahlung (BESSY) using the SX700/II monochromator of the Freie Universität Berlin.[15] The energy resolution ΔE (full width at half maximum) was approximately 200 meV at the O 1*s* edge (~530 eV), 280 meV at the Mn 2*p* edge (~640 eV) and 320 meV at the Fe 2*p* edge (~700 eV). All the spectra were collected in the total-electron-yield mode in a vacuum of better than 5×10^{-10} Torr. The spectra were divided by the yield of a clean Pt sample in order to take possible variations in the throughput of the monochromator into account. The energy scales were calibrated via the known peak positions of TiO_2 and CuO.

The $La_{1-x}Sr_xFeO_3$ samples were prepared by mixing together appropriate molar amounts of La_2O_3, $SrCO_3$, and α-Fe_2O_3. The mixtures were ground and calcined several times and were shaped into rods. They were melted, except for $SrFeO_3$, in a floating-zone furnace under oxygen atmosphere. Finally, they were annealed at 1000 °C under pressure. The $La_{1-x}Sr_xMnO_3$ samples were prepared using a similar procedure. X-ray diffraction showed that the samples were single phase. In order to avoid possible oxygen loss during the baking procedure of the experimental chamber, the samples were introduced just for the measurements by means of a fast-entry-lock system. In addition, all samples were scraped *in situ* with a diamond file to remove surface contaminations. All spectra were taken several times, whereby different parts of the samples were illuminated in order to ensure reproducibility and consistency.

III. RESULTS AND INTERPRETATION

A. Fe 2*p* spectra of $La_{1-x}Sr_xFeO_3$

The Fe 2*p* x-ray absorption spectra of $La_{1-x}Sr_xFeO_3$ for different Sr concentrations are shown in Fig. 1. As throughout this paper, the spectra have been normalized to equal maximum peak heights. The spectra consist of two multiplets, which are separated, to a first approximation, by the spin-orbit splitting of the Fe 2*p* core hole. The spectra can be simulated by calculating the projection of the atomic multiplets in octahedral symmetry, as shown by de Groot *et al.*[11] Such calculation cannot predict absolute energy positions of the multiplets, since it does not properly take into account relaxation and screening effects. In the present case, the absolute energy

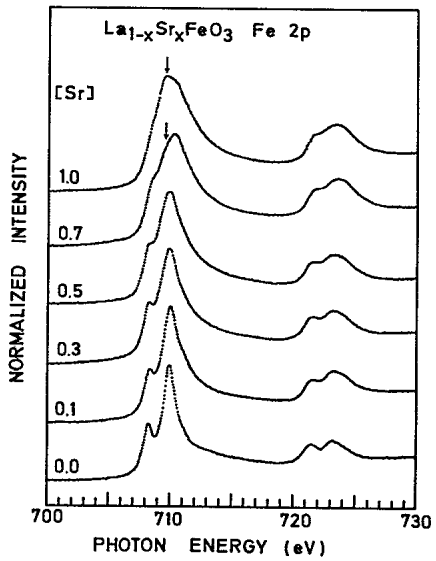

FIG. 1. Fe 2*p* x-ray absorption spectra of $La_{1-x}Sr_xFeO_3$ for various Sr concentrations. The vertical arrows indicate the appearance of a different component for high Sr contents.

scales of the calculated spectra were off by 2–3 eV, so that the multiplets had to be shifted in order to get best agreement with experiment. In addition, the Slater integrals used in the calculations were scaled down to 70% of their atomic values in order to mimic covalency effects.

Before discussing the effects of doping on the spectra, we first analyze the Fe $2p$ spectrum of $LaFeO_3$ presented at the bottom of Fig. 1. This spectrum exhibits particularly sharp multiplets and can be theoretically simulated assuming a high-spin $t_{2g}^3e_g^2$ ($^6A_{1g}$) ground state with $10Dq=1.8$ eV. A comparison between the calculated and experimental spectra is given in Fig. 2(a). This comparison shows clearly that the ground state of $LaFeO_3$ is mainly $3d^5$. In addition, the Fe $2p$ spectrum is similar to equivalent EELS results for α-Fe_2O_3 with Fe^{3+} in octahedral sites.[16–18] It is worth noting that the value of the crystal-field parameter $10Dq$ used in the simulation is in close agreement with the optical value of 1.7 eV obtained for Fe^{3+} in aqueous solution,[19,20] where the Fe ions are also in an approximate octahedral coordination of oxygen ligands.

When one replaces La^{3+} by Sr^{2+} in $La_{1-x}Sr_xFeO_3$, the Fe $2p$ spectra in Fig. 1 become broader. This broadening can be *loosely* attributed to increased covalency in the initial state; a more detailed discussion is given below. It is worth noting, however, that up to $x\approx0.5$, the overall shapes of the multiplets hardly change. This fact indicates that at least in the first half of the series the Fe ions remain essentially in a $3d^5$ configuration. Thus, in order to preserve charge neutrality, the holes induced by doping in $La_{1-x}Sr_xFeO_3$ up to $x\approx0.5$ must necessarily go to states of primarily oxygen character. We conclude that the main component of the ground state in $La_{1-x}Sr_xFeO_3$ for $x\approx0.5$ is $3d^5\underline{L}$ (where $\underline{L}$ denotes a ligand hole) and not $3d^4$. This kind of behavior upon doping is similar to that found in most late-transition-metal oxides.[7]

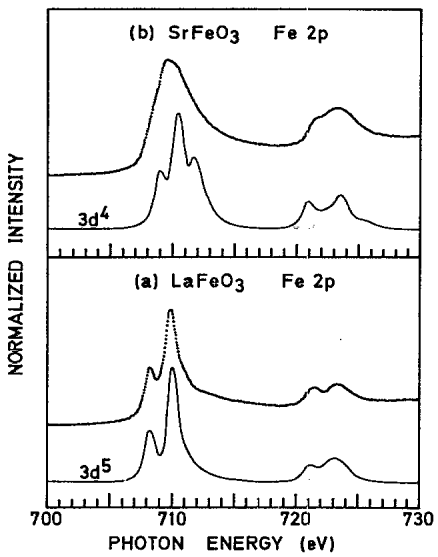

FIG. 2. (a) Comparison between the Fe $2p$ x-ray absorption spectrum of $LaFeO_3$ (dots) and a simulation calculated assuming a $3d^5$ ground state, with $10Dq=1.8$ eV (solid line). (b) Comparison between the Fe $2p$ x-ray absorption spectrum of $SrFeO_3$ (dots) and a simulation calculated assuming a $3d^4$ ground state, with $10Dq=1.8$ eV (solid line).

We observe that the Fe $2p$ spectrum of $La_{0.3}Sr_{0.7}FeO_3$ in Fig. 1 exhibits a distinctive shoulder, marked by a vertical arrow, in the $2p_{3/2}$ region. This component grows even more and dominates the $2p_{3/2}$ region of the spectrum of $SrFeO_3$, although the other features in the spectra are not changing appreciably. There are three possible explanations for the extra peak: (a) the ground state becomes $3d^4$, (b) the ground state becomes a mixture of $3d^5\underline{L}$ and $3d^4$, or (c) the ground state remains essentially $3d^5\underline{L}$, but the $3d^5$ part contains more than one symmetry. It is not possible to decide on these alternatives based on the present data alone. However, we want to make a few remarks based on additional evidence.

The first possibility is very unlikely, since a change in the Fe $3d$ count would give a completely different spectrum with appreciable chemical shifts. These effects are illustrated in the series of calculations performed by de Groot *et al.*[11] as well as by the V $2p$ spectra of several vanadium oxides with different oxidation states of V.[21] To support this argument, the Fe $2p$ spectrum of $SrFeO_3$ and a typical simulation for Fe^{4+}, with $10Dq=1.8$ eV, are compared in Fig. 2(b).[22] It is clear that the disagreement is much too strong to accept a ground state of primarily $3d^4$ character. However, we cannot exclude the possibility that the ground state in $SrFeO_3$ is a mixture of $3d^5\underline{L}$ and $3d^4$. The third possibility cannot be excluded either and will be explored below.

B. O 1*s* spectra of $La_{1-x}Sr_xFeO_3$

The O $1s$ x-ray absorption spectra of $La_{1-x}Sr_xFeO_3$ for different Sr concentrations are presented in Fig. 3. The spectra originate from transitions into unoccupied states with O $2p$ character hybridized with metal states. The structure in the spectra can be qualitatively related to empty bands of primarily metal weight. Unfortunately, a quantitative discussion is presently not possible, since not even a total DOS is available for these compounds. We note that the analysis neglects the effects of the O $1s$ core hole in the final state as well as electron correlations among the valence electrons. Although these effects contribute to the detailed shape of the spectra they do not significantly influence the interpretation.

Before discussing further the effects of doping in the series, we analyze first the O $1s$ spectrum of $LaFeO_3$, displayed in the bottom part of Fig. 3. The shaded doublet above threshold is attributed to bands of minority Fe $3d$ states split by the octahedral crystal field into t_{2g} and e_g orbitals. This assignment is consistent with the schematic Fe $3d$ energy-level diagram of $LaFeO_3$ presented in Fig. 4. According to this assignment, the energy separation between the peaks should directly represent the crystal-field parameter $10Dq$. This results in $10Dq=1.2$ eV, which is smaller than the value of 1.8 eV obtained in the calculation of the Fe $2p$ spectrum. The discrepancy is attributed to the influence of electron

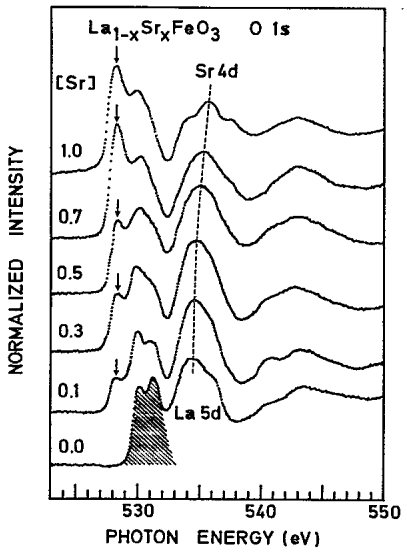

FIG. 3. O 1*s* x-ray absorption spectra of $La_{1-x}Sr_xFeO_3$ for various Sr concentrations. The shaded region in the spectrum of $LaFeO_3$ indicates bands of primarily Fe 3*d* character. The vertical arrows signal a growing prepeak induced by the substitution of La^{3+} by Sr^{2+}. The dashed line illustrates how the La 5*d* related structure in $LaFeO_3$ evolves into Sr 4*d* bands across the series.

correlation and hybridization effects in the final state. Based on the width of the doublet we estimate that the dispersion of the Fe 3*d* bands in $LaFeO_3$ is approximately 1.2–1.4 eV. The broad structure centered around 535 eV is attributed to bands of primarily La 5*d* character. Finally, the structure starting at 540 eV is attributed to bands of higher-energy metal states, like Fe 4*sp* and La 6*sp*. These assignments are consistent with previous XAS and EELS studies of transition-metal compounds[23–27] and with preliminary band-structure calculations for $LaTiO_3$ and $SrTiO_3$.[28]

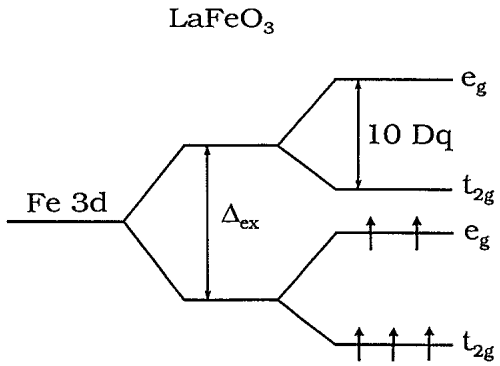

FIG. 4. Schematic diagram of the Fe 3*d* levels in $LaFeO_3$. The levels are split by exchange interactions Δ_{ex} into majority (spin-up) and minority (spin-down) states. Each state is additionally split by the octahedral crystal field, $10Dq$, into t_{2g} (threefold degenerate) and e_g (twofold degenerate) orbitals. The Fe 3*d* electrons are in a high-spin configuration, $t_{2g}^3 e_g^2$ ($^6A_{1g}$), because $\Delta_{ex} > 10Dq$.

Figure 3 shows that substitution of La^{3+} by Sr^{2+} in $La_{1-x}Sr_xFeO_3$ causes two main changes in the spectra. First, we note the appearance of a clearly separated prepeak, marked by means of a vertical arrow, that grows below the absorption threshold of the parent compound and dominates the spectra for high Sr contents. At the same time, the Fe 3*d* doublet, sitting on the high-energy side of the prepeak, is suppressed and changes until it becomes a complex shoulder for $x = 1$. The prepeak can be attributed to transitions to new states which contain O 2*p* character. In some cases, like $Li_xNi_{1-x}O$,[8] these *effective* states are even pinned by the impurity potential at the dopant site. The character of these states is very difficult to determine unless one resorts to rather involved theoretical calculations.[29–31] In general, it would be premature to conclude directly that these states are primarily made up of O 2*p* character without a detailed model calculation. In fact, we reached this conclusion indirectly, in the analysis of the Fe 2*p* spectra, and only for low Sr contents. Figure 3 shows that the intensity of the prepeak increases steadily in the series up to $SrFeO_3$, see Fig. 3. This fact seems to support the idea that the Fe ions remain essentially $3d^5$, even for high Sr concentrations. However, the intensity of the prepeak cannot be related directly to the amount of holes at the O sites.

The second change observed in Fig. 3 concerns the structure related to La 5*d* states in $LaFeO_3$. This structure changes its shape and shifts towards higher energies as one replaces La^{3+} by Sr^{2+}. This evolution, indicated by the dashed line in Fig. 3, is attributed to the change from bands of La 5*d* to bands of Sr 4*d* character. This crossover behavior is characteristic of all $La_{1-x}Sr_xMO_3$ oxides and will be found again in the O 1*s* spectra of $La_{1-x}Sr_xMnO_3$. The assignment is also consistent with preliminary band-structure calculations for $LaTiO_3$ and $SrTiO_3$.[28] There are also some changes in the higher-energy metal bands at energies above 540 eV; these changes are less relevant to the topics addressed here and will therefore not be discussed further.

C. Mn 2*p* spectra of $La_{1-x}Sr_xMnO_3$

The Mn 2*p* x-ray absorption spectra of $La_{1-x}Sr_xMnO_3$ for various Sr concentrations are shown in Fig. 5. The spectra present two broad multiplets separated, in a first approximation, by the spin-orbit splitting of the Mn 2*p* core hole. We note that the broadening of the spectral lines is not an experimental artifact but rather of intrinsic origin. In particular, the spectrum of $LaMnO_3$ in Fig. 5 is considerably less resolved than the Fe 2*p* spectra of $LaFeO_3$ in Fig. 1. This additional broadening is due to several contributions. The main contribution to the broadening is the larger Mn 3*d* bandwidth in $LaMnO_3$, as estimated below from the O 1*s* XAS spectrum. Other contributions include a more covalent character of the ground state than in $LaFeO_3$ and a larger spread of the multiplet induced by the lower symmetry around the Mn ions.

The Mn 2*p* spectrum of $LaMnO_3$ can be theoretically simulated assuming a $t_{2g}^3 e_g$ (^5E_g) ground state with

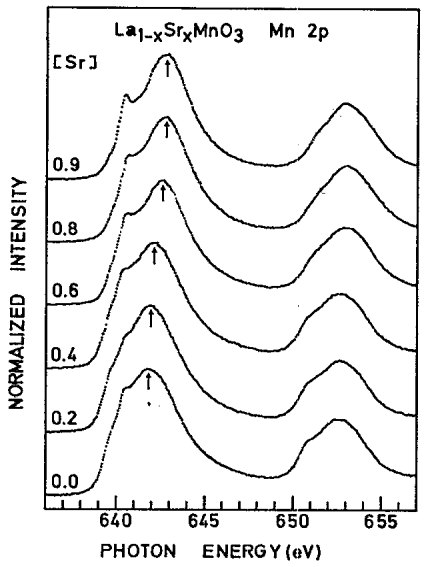

FIG. 5. Mn $2p$ x-ray absorption spectra of $La_{1-x}Sr_xMnO_3$ for various Sr concentrations. The vertical arrows show how the maximum of the $2p_{3/2}$ multiplet shifts from 641.8 eV in $LaMnO_3$ to 642.8 eV in $La_{0.1}Sr_{0.9}MnO_3$.

$10Dq=1.5$ eV. A comparison between the calculated and the experimental spectra is presented in Fig. 6(a). The agreement is not completely good because the calculation did not take into account lower symmetry effects. This comparison shows that the main component of the ground state in $LaMnO_3$ is $3d^4$. In addition, the spectrum is similar to the Mn $2p$ EELS results of Mn_2O_3, with Mn^{3+} in a slightly distorted octahedral symmetry.[18]

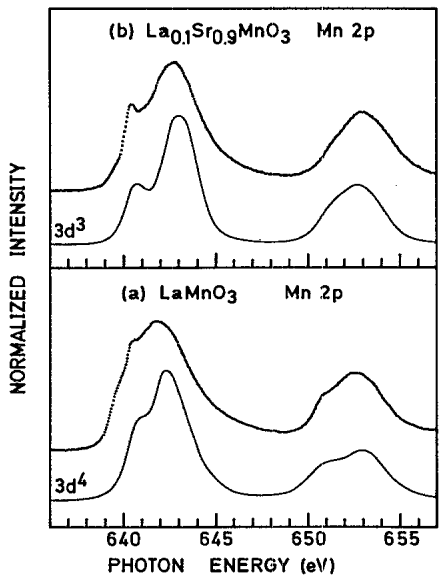

FIG. 6. (a) Comparison between the Mn $2p$ x-ray absorption spectrum of $LaMnO_3$ (dots) and a simulation calculated assuming a $3d^4$ ground state with $10Dq=1.5$ eV (solid line). (b) Comparison between the Mn $2p$ x-ray absorption spectrum of $La_{0.1}Sr_{0.9}MnO_3$ (dots) and a simulation calculated assuming a $3d^3$ ground state with $10Dq=2.4$ eV (solid line).

Figure 5 shows that as one replaces La^{3+} by Sr^{2+} in $La_{1-x}Sr_xMnO_3$, the Mn $2p$ spectra change shape and shift towards higher energies. In particular, the maximum of the Mn $2p_{3/2}$ multiplet in Fig. 5, marked by vertical arrows, moves from 641.8 eV in $LaMnO_3$ to 642.8 eV in $La_{0.1}Sr_{0.9}MnO_3$. These effects are both relevant, because they indicate a decrease in the $3d$ count at the Mn site. The change of shape is expected due to the sensitivity of the transition-metal spectra to the symmetry of the ground state.[11] The chemical shift is caused by changes in the electrostatic energy at the Mn site driven by the decrease in the $3d$ count. These shifts were previously used to study site-specific valence determination in EELS studies of transition-metal oxides.[32]

The Mn $2p$ spectrum of $La_{0.1}Sr_{0.9}MnO_3$ can be theoretically simulated assuming a t_{2g}^3 ($^4A_{2g}$) ground state with $10Dq=2.4$ eV. A comparison between the calculated and experimental spectra is illustrated in Fig. 6(b). In addition, the spectrum is quite similar to the Mn $2p$ EELS results of MnO_2, with Mn^{4+} in octahedral symmetry.[18] All these facts indicate that the holes induced by substitution in the $La_{1-x}Sr_xMnO_3$ series go to states which contain an appreciable amount of Mn $3d$ character. That would suggest that the ground state for high Sr contents becomes $3d^3$. However, we show below, by using the O $1s$ XAS spectra, that these states contain also considerable O $2p$ character. We will finally conclude that the ground state of $SrMnO_3$ is a mixture of $3d^3$ and $3d^4\underline{L}$.

D. O 1s spectra of $La_{1-x}Sr_xMnO_3$

The O $1s$ x-ray absorption spectra of $La_{1-x}Sr_xMnO_3$ for various Sr concentrations are shown in Fig. 7. The O $1s$ spectrum of $LaMnO_3$ presents features which are similar to those discussed in the spectrum of $LaFeO_3$. The

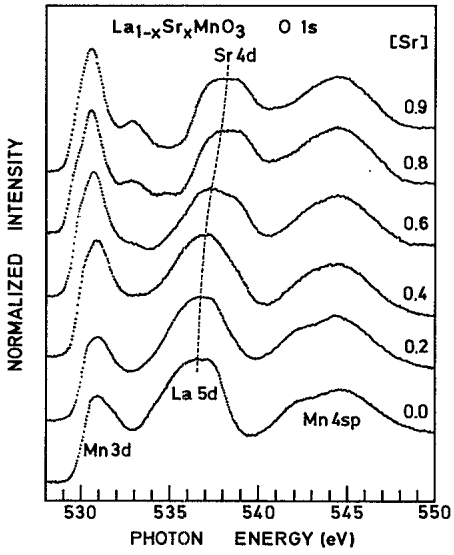

FIG. 7. O $1s$ x-ray absorption spectra of $La_{1-x}Sr_xMnO_3$ for various Sr concentrations. The labels in the $LaMnO_3$ spectrum indicate the main character of each structure. The dashed line illustrates how the La $5d$ related structure in $LaMnO_3$ evolves into Sr $4d$ bands with increasing x.

broad structure centered at 531 eV is attributed to overlapping bands of Mn 3*d* related character; a more detailed account is given below. The dispersion of the Mn 3*d* bands derived from this structure is 1.8–2.0 eV. This bandwidth is larger than the Fe 3*d* bandwidth of $LaFeO_3$, which helps to explain the larger broadening observed in the Mn 2*p* spectra. The broad structure centered at 536.5 eV is attributed to bands of La 5*d* character, while the structure above 540 eV is due to higher-energy metal states, like Mn 4*sp* and La 6*sp*. These assignments are consistent with preliminary band-structure calculations for $LaTiO_3$ and $SrTiO_3$.[28]

Figure 7 shows that replacement of La^{3+} by Sr^{2+} in $La_{1-x}Sr_xMnO_3$ causes several changes in the O 1*s* spectra. In contrast to $La_{1-x}Sr_xFeO_3$, no prepeak is observed to emerge below the threshold of the parent compound. However, the spectra show clearly that the intensity of the structure related to bands of Mn 3*d* character increases strongly in the series. This fact indicates not only more unoccupied O 2*p* character, but also that this character is heavily mixed to Mn 3*d* states. We then conclude that the holes induced by substitution in $La_{1-x}Sr_xMnO_3$ go to states of heavily mixed metal-ligand character.

Figure 7 also shows that for higher Sr contents a second band of Mn 3*d* character appears at 533 eV. The first structure is assigned to an accidental superposition of majority e_g and minority t_{2g} bands, since in this case the exchange splitting Δ_{ex} is only slightly larger than the crystal-field splitting $10Dq$. On the other hand, the second structure at 533 eV is attributed to a band of minority e_g character. These assignments are consistent with the Mn 3*d* energy-level for $SrMnO_3$ illustrated schematically in Fig. 8. Taking this diagram into account, it is clear that the of $LaMnO_3$. This Mn 3*d* band is hidden in the low-energy tail of the La 5*d* band for small *x*.

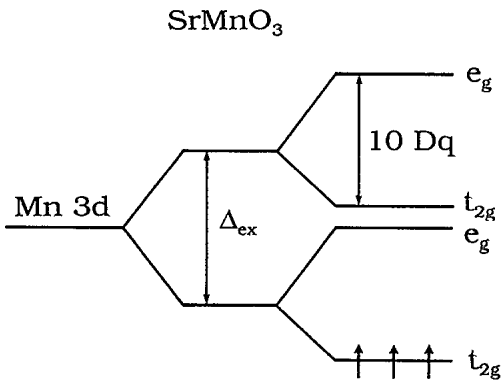

FIG. 8. Schematic diagram of the Mn 3*d* levels in $SrMnO_3$. The levels are split by exchange interactions Δ_{ex} into majority (spin-up) and minority (spin-down) states. Each state is additionally split by the octahedral crystal field $10Dq$ into t_{2g} (threefold degenerate) and e_g (twofold degenerate) orbitals. The Mn 3*d* electrons are in a high-spin configuration, t_{2g}^3 ($^4A_{2g}$). The majority e_g and minority t_{2g} orbitals are almost degenerate because, in this case, Δ_{ex} is only slightly larger than $10Dq$.

Another change observed in the spectra of Fig. 7 concerns the evolution of the structure related to La 5*d* states in $LaMnO_3$ indicated by the dashed line. As in $La_{1-x}Sr_xFeO_3$, this structure changes shape and shifts towards higher energies when La^{3+} is replaced by Sr^{2+}. Accordingly, these effects are also attributed to the crossover from bands of La 5*d* to bands of Sr 4*d* character. Finally, the changes observed above 540 eV involve higher-energy metal states, like Mn 4*sp*, and are less relevant for the analysis of ground-state properties. These assignments are consistent with those made for $La_{1-x}Sr_xFeO_3$ and with preliminary band-structure calculations.[28]

IV. DISCUSSION

A. Trends in controlled-valence properties

Based on the analysis of the spectra, we concluded that the holes induced by substitution in $La_{1-x}Sr_xFeO_3$ go to states of mixed character with primarily O 2*p* weight for low Sr contents. In $La_{1-x}Sr_xMnO_3$ the extra holes go to states of heavily mixed Mn 3*d*–O 2*p* character. The ground state and the 3*d* symmetry of the end members of the series are summarized in Table I. These conclusions are in qualitative agreement with those obtained in x-ray photoelectron spectroscopy (XPS) studies of similar materials performed by Bocquet *et al.*[33]

As expected, the intermediate cases presented here bridge the opposite behavior upon hole doping of early- and late-transition-metal oxides. We want to discuss now the origin of this contrasting behavior. The main question is why the $3d^n$ ground state of the parent compound becomes $3d^{n-1}$ in one case and $3d^n\underline{L}$ in the other. To this end, it is necessary to compare the Mott-Hubbard energy U (needed to transfer a 3*d* electron from one transition-metal ion to a neighboring one) (Refs. 34 and 35) with the charge-transfer energy Δ (needed to transfer one electron from the ligand band to the transition-metal site).[36–38] These parameters determine the ordering of the first excited energy levels in the solid, as described by the Zaanen-Sawatzky-Allen (ZSA) model.[39,40] Table II summarizes the first ionization and affinity states of a solid with a $3d^n$ ground state according to this model. There are three possibilities depending on the relative magnitude of U and Δ.

For low Sr concentrations and neglecting the influence of the impurity potential, the holes induced by substitution will go to the first ionization states of the solid.[41] This fact allows one to rationalize the controlled-valence

TABLE I. Summary of the main components of the ground state and of the main symmetry of the 3*d* part of the ground states for the end members of the $La_{1-x}Sr_xFeO_3$ and $La_{1-x}Sr_xMnO_3$ series of compounds.

Compound	Ground state	3*d* symmetry
$LaFeO_3$	$3d^5$	$^6A_{1g}$
$SrFeO_3$	$3d^5\underline{L}$	$^6A_{1g}$
$LaMnO_3$	$3d^4$	^5E_g
$SrMnO_3$	$3d^3+3d^4\underline{L}$	$^4A_{2g}$

TABLE II. First ionization and affinity states of a solid with a $3d^n$ ground state according to the Zaanen-Sawatzky-Allen model. The different possibilities are classified according to the relative value of the Mott-Hubbard U and the charge-transfer energy Δ.

	Ground state	First ionization state	First affinity state
$U>\Delta$	$3d^n$	$3d^n\underline{L}$	$3d^{n+1}$
$U<\Delta$	$3d^n$	$3d^{n-1}$	$3d^{n+1}$
$U\approx\Delta$	$3d^n$	mixed	$3d^{n+1}$

properties of all transition-metal compounds in terms of the classification scheme provided by the ZSA model. For $U>\Delta$ these states will be mainly $3d^n\underline{L}$, as in the $La_{1-x}Sr_xFeO_3$ series for low Sr contents. For $U<\Delta$ the states will be mainly $3d^{n-1}$, as in most early transition-metal oxides.[7] Finally, for $U\approx\Delta$ the states will be of heavily mixed character, as in the $La_{1-x}Sr_xMnO_3$ series. The opposite behavior upon hole doping across the transition-metal oxide series is the consequence of differences in the relative magnitude of U and Δ in the parent compounds.

B. Covalent broadening in the Fe 2p spectra of $La_{1-x}Sr_xFeO_3$

Figure 1 shows that replacement of La by Sr in $La_{1-x}Sr_xFeO_3$ induces a broadening of the spectral features in the Fe $2p$ spectra. This extra broadening was loosely attributed to an increase in the covalent character of the ground state. A more precise description of this effect in the case of the Ni $2p$ XAS spectra of $Li_xNi_{1-x}O$ was recently offered by van Elp *et al.*[42] Here, we use similar arguments to explain the extra broadening in the Fe $2p$ spectra of the $La_{1-x}Sr_xFeO_3$ series. The main component of the $LaFeO_3$ ground state is high-spin $3d^5$, which in octahedral field becomes $t_{2g}^3e_g^2$ with total symmetry given by the term symbol $^6A_{1g}$.[43–46] As La^{3+} is replaced by Sr^{2+} the holes go to states of primarily O $2p$ character and the main component of the ground state become $3d^5\underline{L}$. The total symmetry of the ground state Γ_{GS} is equal to $\Gamma_{3d}\times\Gamma_L$, where Γ_{3d} is the symmetry of the $3d^5$ part and Γ_L is the symmetry of the ligand hole part. The total symmetry Γ_{GS} is in general unique. However, we note that Γ_{3d} is no longer a pure $^6A_{1g}$ state, since the presence of the ligand hole allows small admixtures of other symmetries. In turn, each of these symmetries gives rise to a different Fe $2p$ multiplet, as illustrated in Fig. 9. Therefore the total spectrum is really a mixture with several secondary components, and the overall effect of these smaller components is an increase in broadening.

C. Origin of the extra peak in the Fe 2p spectra of $SrFeO_3$

Figure 1 shows that the Fe $2p$ spectra of $La_{1-x}Sr_xFeO_3$ for high Sr concentrations contains an extra peak marked by vertical arrows. The origin of this extra peak might be explained following the same argument outlined in the preceding paragraph. The main component of the ground state in $LaFeO_3$ is $3d^5$ with $^6A_{1g}$ symmetry. As La^{3+} is replaced by Sr^{2+} in $La_{1-x}Sr_xFeO_3$, the main component of the ground state becomes $3d^5\underline{L}$. For small Sr contents, the main symmetry of the $3d^5$ part of the ground must still be $^6A_{1g}$. Otherwise, the Fe $2p$ spectra would have shown extensive changes, which is not observed. For higher Sr contents small admixtures of secondary Γ_{3d} symmetries are allowed by the presence of the ligand hole. We suggest that in $SrFeO_3$ one of the secondary Γ_{3d} symmetries might attain enough weight to generate the extra peak observed in the Fe $2p$ spectrum. In particular, Fig. 9 shows that the multiplets generated by some of the first excited terms contains weight in the region where the extra peak appears.

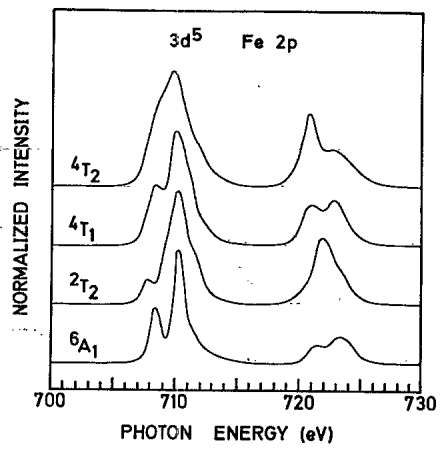

FIG. 9. Simulations of the Fe $2p$ x-ray absorption spectra for various initial state symmetries. The spectra were calculated assuming a $3d^5$ ground state with $10Dq=1.8$ eV. The spectra are shown in order of increasing initial state energy; the ground-state symmetry of $LaFeO_3$ is $^6A_{1g}$. For high Sr contents, the $3d^5$ part of the $3d^5\underline{L}$ ground state becomes a mixture of different symmetries.

V. SUMMARY AND CONCLUSIONS

In summary, we presented high-resolution oxygen $1s$ and transition-metal $2p$ x-ray absorption spectra of $La_{1-x}Sr_xFeO_3$ and $La_{1-x}Sr_xMnO_3$. The transition-metal $2p$ spectra are compared to atomic-multiplet simulations in order to determine the valency of such ions. The Fe $2p$ spectrum of $LaFeO_3$ is consistent with a $3d^5$ ($^6A_{1g}$) ground state. The Fe $2p$ spectra of the $La_{1-x}Sr_xFeO_3$ series for low Sr concentrations remain essentially unchanged, but for higher Sr contents a second component appears in the spectra. The O $1s$ spec-

tra of $La_{1-x}Sr_xFeO_3$ show a strong prepeak growing below the bottom of the conduction band of $LaFeO_3$. We conclude that the holes induced by substitution in this series go to states of mixed Fe $3d-O\ 2p$ character. However, for low Sr contents these states are primarily made up of O $2p$ weight. The Mn $2p$ spectra of the $La_{1-x}Sr_xMnO_3$ series present changes which are attributed to a decrease in the Mn $3d$ count. In this case, the O $1s$ spectra also show changes related to more unoccupied O $2p$ character mixed in with Mn $3d$ states. We conclude that the holes induced by substitution in this series go to states of heavily mixed character. The contrasting behavior upon doping of early- and late-transition-metal oxides can be rationalized within the framework of the ZSA model.

ACKNOWLEDGMENTS

We thank the technical and scientific staff of the Berliner Elektronen Speicherring-Gesellschaft für Synchrotronstrahlung (BESSY) and especially W. Braun. This work was partially supported by Fundamenteel Onderzoek der Materie (FOM) and Scheikundig Onderzoek Nederland (SON). The research of the Berlin group was supported by the Bundesminister für Forschung und Technologie, project 05-473 AXI-7/TP4, and the Deutsche Forschungsgemeinschaft, project Ka 564/2-1. The cooperation between the different groups was made possible by grants from the European Community, through the Science and Large Scale Installation programs.

[1]J. B. Goodenough, *Magnetism and the Chemical Bond* (Wiley, New York, 1963).
[2]M. B. Robin and P. Day, Adv. Inorg. Chem. Radiochem. **10**, 247 (1967).
[3]J. B. Goodenough, in *Progress in Solid State Chemistry,* edited by H. Reiss (Pergamon, Oxford, 1971), Vol. 5, p. 145.
[4]C. N. R. Rao and J. Gopalakrishnan, *New Directions in Solid State Chemistry* (Cambridge University Press, Cambridge, 1986).
[5]*Unoccupied Electronic States,* edited by J. C. Fuggle and J. E. Inglesfield (Springer, Berlin, 1991).
[6]J. C. Fuggle, J. Fink, and N. Nücker, Int. J. Mod. Phys. B **1**, 1185 (1988); F. Al Shamma and J. C. Fuggle, Physica C **169**, 325 (1990).
[7]M. Abbate, F. M. F. de Groot, J. C. Fuggle, A. Fujimori, Y. Tokura, Y. Fujishima, O. Strebel, M. Domke, G. Kaindl, J. van Elp, B. T. Thole, G. A. Sawatzky, M. Sacchi, and N. Tsuda, Phys. Rev. B **44**, 5419 (1991).
[8]P. Kuiper, G. Kruizinga, J. Ghijsen, and G. A. Sawatzky, Phys. Rev. Lett. **62**, 221 (1989).
[9]P. Kuiper, J. van Elp, G. A. Sawatzky, A. Fujimori, S. Hosoya, and D. M. de Leeuw, Phys. Rev. B **44**, 4570 (1991).
[10]J. van Elp, H. Eskes, P. Kuiper, and G. A. Sawatzky, Phys. Rev. B **45**, 1612 (1992).
[11]F. M. F. de Groot, J. C. Fuggle, B. T. Thole, and G. A. Sawatzky, Phys. Rev. B **41**, 928 (1990); **42**, 5457 (1990).
[12]M. Pedio, J. C. Fuggle, J. Somers, E. Umbach, J. Haase, Th. Linder, U. Höfer, M. Grioni, F. M. F. de Groot, B. Hillert, L. Becker, and A. Robinson, Phys. Rev. B **40**, 7924 (1990).
[13]M. Grioni, M. T. Czyzyk, F. M. F. de Groot, J. C. Fuggle, and B. E. Watts, Phys. Rev. B **39**, 4886 (1990).
[14]For a complete compilation of properties see, for example, J. B. Goodenough and J. M. Longo, Landolt-Börnstein Tabellen, New Series, Vol. III/4a (Springer, Berlin, 1970).
[15]M. Domke, C. Xue, A. Puschmann, T. Mandel, E. Hudson, D. A. Shirley, and G. Kaindl, Chem. Phys. Lett. **173**, 122 (1990).
[16]K. M. Krishnan, Ultramicroscopy **32**, 309 (1990).
[17]O. L. Krivanek and J. H. Paterson, Ultramicroscopy **32**, 313 (1990).
[18]J. H. Paterson and O. L. Krivanek, Ultramicroscopy **32**, 319 (1990).
[19]C. K. Jørgensen, *Absorption Spectra and Chemical Bonding in Complexes* (Pergamon, Oxford, 1962).
[20]C. K. Jørgensen, in *Advances in Chemical Physics,* edited by I. Prigogine (Wiley, New York, 1962), Vol. 5, p. 33.
[21]M. Abbate *et al.* (unpublished).
[22]Simulations calculated with other values of $10Dq$ were also tried but they do not give a better agreement.
[23]D. W. Fischer, J. Appl. Phys. **41**, 3561 (1970); J. Phys. Chem. Solids **32**, 2455 (1971); Phys. Rev. B **5**, 4219 (1972).
[24]L. A. Grunes, R. D. Leapman, C. N. Wilker, R. Hoffmann, and A. B. Kunz, Phys. Rev. B **25**, 7157 (1982); R. D. Leapman, L. A. Grunes, and P. L. Fejes, *ibid.* **26**, 614 (1982); L. A. Grunes, *ibid.* **27**, 2111 (1983).
[25]J. Pflüger, J. Fink, G. Crecelius, K. P. Bohnen, and H. Winter, Solid State Commun. **44**, 489 (1982); J. Pflüger, J. Fink, and K. Schwarz, *ibid.* **55**, 675 (1985).
[26]F. M. F. de Groot, M. Grioni, J. C. Fuggle, J. Ghijsen, G. A. Sawatzky, and H. Petersen, Phys. Rev. B **40**, 5715 (1989).
[27]M. Abbate, F. M. F. de Groot, J. C. Fuggle, Y. J. Ma, C. T. Chen, F. Sette, A. Fujimori, Y. Ueda, and K. Kosuge, Phys. Rev. B **43**, 7263 (1991).
[28]F. M. F. de Groot *et al.* (unpublished).
[29]C. T. Chen, F. Sette, Y. Ma, M. S. Hybertsen, E. B. Stechel, W. M. C. Foulkes, M. Schulter, S.-W. Cheong, A. S. Cooper, L. W. Rupp, B. Batlogg, Y. L. Soo, Z. H. Ming, A. Krol, and Y. H. Kao, Phys. Rev. Lett. **66**, 104 (1991).
[30]E. Dagotto, A. Moreo, F. Ortolani, J. Riera, and D. J. Scalapino, Phys. Rev. Lett. **67**, 1918 (1991).
[31]H. Eskes, M. B. J. Meinders, and G. A. Sawatzky, Phys. Rev. Lett. **67**, 1035 (1991).
[32]J. Taftø and O. L. Krivanec, Phys. Rev. Lett. **48**, 560 (1982).
[33]A. E. Bocquet, T. Mizokawa, T. Saitoh, H. Namatame, and A. Fujimori, Phys. Rev. B (to be published).
[34]N. F. Mott, Proc. Phys. Soc. London, Sect. A **62**, 416 (1949).
[35]J. Hubbard, Proc. R. Soc. London, Ser. A **276**, 238 (1963).
[36]G. A. Sawatzky and J. W. Allen, Phys. Rev. Lett. **53**, 2339 (1984).
[37]A. Fujimori and F. Minami, Phys. Rev. B **30**, 957 (1984).
[38]S. Hüfner, F. Hulliger, J. Osterwalder, and T. Riesterer, Solid State Commun. **50**, 83 (1984).
[39]J. Zaanen, G. A. Sawatzky, and J. W. Allen, Phys. Rev. Lett. **55**, 418 (1985); J. Magn. Magn. Mater. **54**, 607 (1986).
[40]J. Zaanen and G. A. Sawatzky, Can. J. Phys. **65**, 1262 (1987); J. Solid State Chem. **88**, 8 (1990).
[41]One must also take into account that, in some cases, the first

ionization state might not be reachable by means of a one-particle excitation. See, for example, J. van Elp, H. Eskes, and G. A. Sawatzky (unpublished).

[42]J. van Elp, B. G. Searle, G. A. Sawatzky, and M. Sacchi, Solid State Commun. **80**, 67 (1991).

[43]C. J. Ballhausen, *Introduction to Ligand Field Theory* (McGraw-Hill, New York, 1962).

[44]B. N. Figgis, *Introduction to Ligand Fields* (Wiley, New York, 1966).

[45]S. Sugano, Y. Tanabe, and H. Kamimura, *Multiplets of Transition-Metal Ions in Crystals* (Academic, New York, 1970).

[46]J. S. Griffith, *The Theory of Transition Metal Ions* (Cambridge University Press, Cambridge, 1961).